JCTC Journal of Chemical Theory and Computation

Article

pubs.acs.org/JCTC

Performance of Density Functionals for Activation Energies of Re-Catalyzed Organic Reactions

Yihua Sun and Hui Chen*

Beijing National Laboratory for Molecular Sciences (BNLMS), CAS Key Laboratory of Photochemistry, Institute of Chemistry, Chinese Academy of Sciences, Beijing, 100190, China

Supporting Information

ABSTRACT: By employing high-level coupled cluster CCSD(T)-F12 calculations as reference, we herein systematically assessed the performance of 16 popular density functional theory (DFT) approximations for typical rhenium-catalyzed reactions. The reactions under study cover those catalyzed by low-valent rhenium(I)/(III) carbonyl complexes as well as high-valent organorhenium(VII) bisperoxo complex. Without DFT dispersion correction, the four best-performing functionals for the barrier heights are B2GP-PLYP, TPSSh, B3LYP, and PBE0 with the mean unsigned deviations (MUDs) under 1.6 kcal/mol. Among these four functionals, B2GP-PLYP generates more accurate barrier heights, while B3LYP and TPSSh behave more reliably in the barrier trend description for these Re-catalyzed reactions. In general, herein the hybrid functionals are better choices than pure GGA or pure meta-GGA functionals. DFT empirical dispersion corrections were found to have beneficial effects on MUDs only for four tested functionals of BMK, CAM-B3LYP, LC-ωPBE, and ωB97X. Often associated with very large errors up to about 15 kcal/mol in barrier height for many tested functionals, the reaction catalyzed by high-valent rhenium(VII) bisperoxo is apparently different from the ones catalyzed by low-valent rhenium(I)/(III) carbonyl complexes. For reactions catalyzed by Re(I)/(III) carbonyl complexes, ωB97XD with dispersion correction performs excellently (MUD = 0.63 kcal/mol) and hence is highly recommended for these Re(I)/Re(III)-mediated reactions.

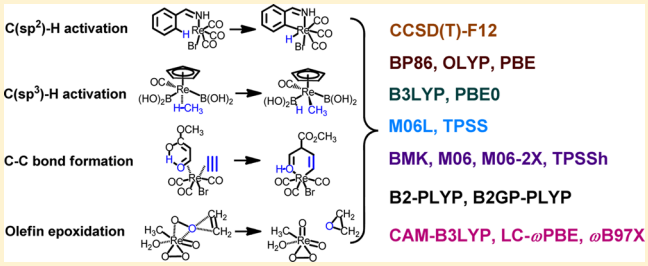

1. INTRODUCTION

Among middle transition metals (Mn, Tc, Re, Fe, Ru, Os), rhenium is a useful one in metal-catalyzed organic reactions. The extensive studies in recent years have revealed its rich and often special catalysis chemistry, from which many new organic transformations have been discovered and developed.[1] Rhenium carbonyl complexes, such as $[ReBr(CO)_3(thf)]_2$, $Re(CO)_5Br$, $Re(CO)_5Cl$, $Re_2(CO)_{10}$, and $[Cp^*Re(CO)_3]$, account for a significant portion of known rhenium complexes generated from synthesis.[2] Rhenium carbonyl complexes are featured by the ability to activate $C(sp^2)$-H and $C(sp^3)$-H bonds, which allows for introduction of various functional groups or substituents directly into C−H bonds (reactions 1 and 2 in Scheme 1).[3−8] As shown in reaction 1, after the first crucial step of Re-mediated $C(sp^2)$-H activation (reaction 1a) through oxidative addition, the insertion of many polar and nonpolar unsaturated molecules into the Re−C bond, such as acetylenes,[3,4] isocyanates,[4] aldehydes,[5] and acrylates,[6] can be followed. The successive intramolecular nucleophilic cyclization would complete the C−H functionalization in the catalytic cycle. In 1999, Hartwig et al. reported that a rhenium(I) carbonyl complex, $Cp^*Re(CO)_3$, is capable of catalyzing $C(sp^3)$-H borylation at the terminal positions of alkanes under photochemical conditions (reaction 2 in Scheme 1, CO ligands can dissociate upon photolysis to open vacant coordinate positions on Re).[8] On the basis of their experimental data, Hartwig et al. proposed that in the borylation of alkanes (R-H), C−H activation starting from the $Cp^*Re^{III}(CO)(R\text{-}H)(Bpin)_2$ intermediate (Bpin =4,4,5,5-tetramethyl-1,3,2-dioxaborolane-2-yl) occurs by either σ-bond metathesis mechanism through Re^{III} or oxidative addition mechanism through Re^{V}. Through DFT calculations, however, we here find that this C−H activation step is more likely to proceed by σ-bond metathesis mechanism, because the intermediate $Cp^*Re^{V}(CO)(R)(H)(Bpin)_2$ after oxidative addition is not a minimum on the potential energy surface. Saturated hydrocarbons like isopentane, methylcyclohexane, and *n*-pentane were found to be reactive in C−H activation, while for methane that bears extremely strong C−H bond, its C−H activation was not reported with $[Cp^*Re(CO)_3]$.

Another feature of rhenium carbonyl complex is their soft Lewis acidity for activation of unsaturated hydrocarbons such as alkynes, alkenes, and allenes. It was reported that a rhenium complex derived from dinuclear $[ReBr(CO)_3(thf)]_2$ can catalyze the insertion of alkynes into the C^{β}-C^{γ} single bond of β-keto esters (reaction 3a,b in Scheme 1).[9] Interestingly, the same combination of substrates and catalyst in this reaction can also catalyze the insertion of terminal alkynes into the C^{β}-H bond of the active methylene group in β-keto esters under

Received: September 30, 2013
Published: December 23, 2013

   dx.doi.org/10.1021/ct4010855 | J. Chem. Theory Comput. 2014, 10, 579−588

Scheme 1. Reactions Studied in This Work

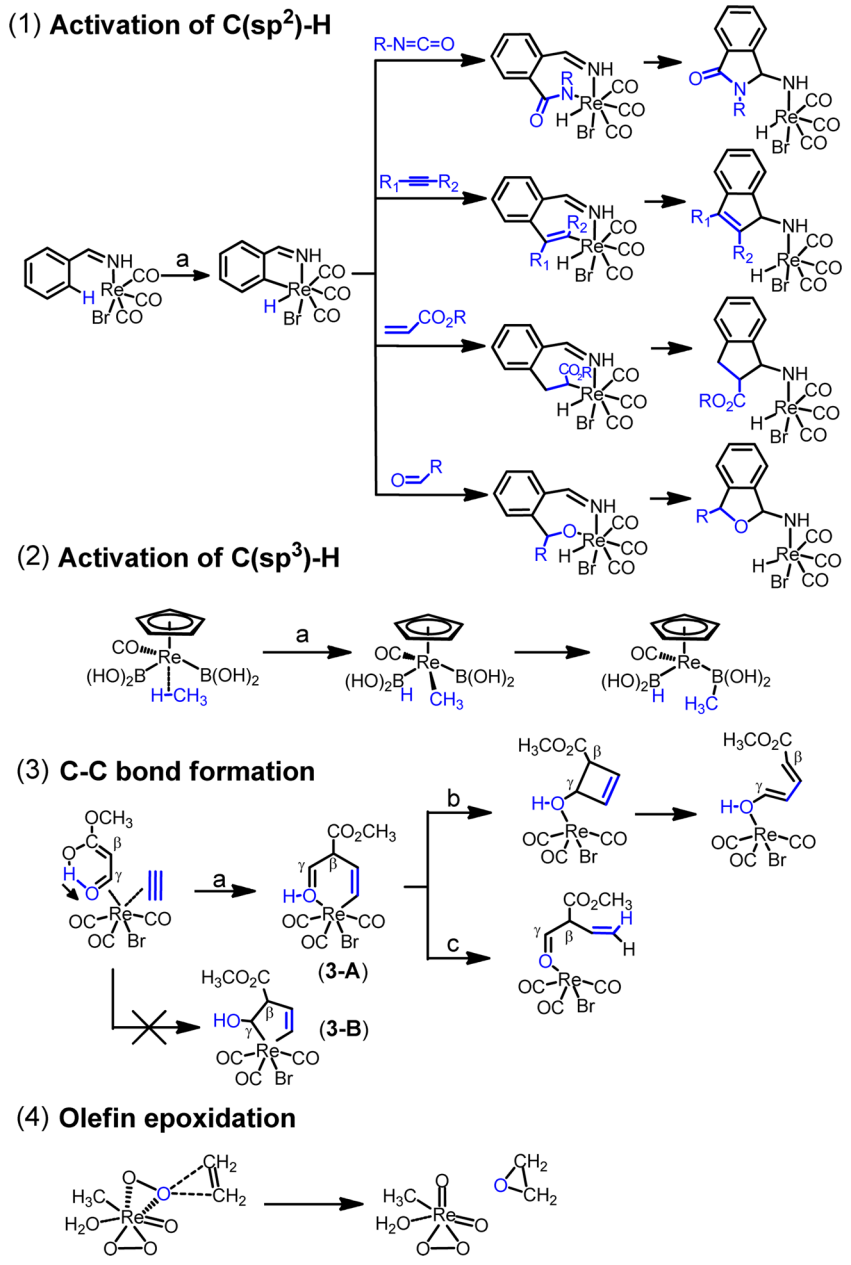

slightly different experimental conditions (reaction 3a,c in Scheme 1).[10] The reaction mechanisms for these reactions proposed by Takai et al., who discovered these two reactions, are featured by formation of either two type of intermediates, i.e. alkenylrhenium (**3-A**) or rhenacyclopentene (**3-B**) as shown in reaction 3 of Scheme 1.[9,10] These two intermediates are all presumably generated from the cycloaddition of rhenium catalyst, enol form of β-keto ester, and terminal alkyne. After some DFT calculations at the B3LYP/cc-pVTZ level, we find here however, that the rhenacyclopentene intermediate **3-B** and the transition state to generate it are more unfavorable in energy by 38.6 and 10.6 kcal/mol, when compared with the corresponding alkenylrhenium species (for details see the Supporting Information). Thus we infer that for these two reactions, the alkenylrhenium pathway is more reasonable than the rhenacyclopentene one. After this point of the alkenylrhenium intermediate **3-A**, the subsequent different steps of intramolecular nucleophilic cyclization and hydrogen migration will lead finally to different routes in two reactions.

Besides the above reactions involving low-valent rhenium(I)/(III) carbonyl complexes, high-valent rhenium-oxo complexes also have their usage in catalytic organic reactions.[11−14] Organorhenium(VII) oxides, most notably methyltrioxorhenium (MTO) $MeReO_3$ have gained special importance as a catalyst for olefin oxidation reaction (reaction 4 in Scheme 1). Although the mechanism of oxygen transfer reaction has been the topic of a debate,[14] a concerted mechanism was favored and suggested by Rösch and Gandolfi et al. based on their computational study,[13] in which the electron rich double bond of the alkene attacks a peroxidic oxygen of $(CH_3)Re(O_2)_2O\cdot H_2O$, a bisperoxo complex generated by the reaction of MTO with excess H_2O_2.

Density functional theory (DFT) methods have been widely used in the transition metal chemistry area and have achieved

dx.doi.org/10.1021/ct4010855 | J. Chem. Theory Comput. 2014, 10, 579−588

significant success.[15−25] The computational efficiency of DFT and its black-box feature in usage have enabled both computational and experimental chemists to explore reaction mechanisms relatively conveniently, in which the kinetic parameters such as reaction barriers are of crucial importance. The development of DFT has offered chemists a great variety of approximate density functionals (DFs). However, the performances of many currently available approximate DFs are often diverse for the same transition metal-mediated reaction. As such, high level ab initio methods such as a coupled cluster (CC) approach often serve as benchmark tools for the calibration and selection of the suitable DFT methods.[26−78] Our previous DFT calibration studies on reaction barriers have been focused on early transition metal of Zr[76] (Group 4), middle transition metals of Ru[75] and Fe[71] (Group 8), and late transition metals of Rh,[74] Pd,[74] Pt,[73,74] Ir,[73,74] and Au.[72,73] In this work, we extend our DFT calibration research of middle transition metals to Group 7 element Re. To the best of our knowledge, the sole DFT calibration study on rhenium complexes is a very recent work by Chan and Ball, in which the molecular geometries and the methane binding energy for the carbonyl Re-methane σ-complex of $CpRe(CO)_2(CH_4)$ were examined.[59] So far a systematic DFT calibration study on the rhenium-catalyzed reaction barriers is still missing. It is the goal of this study to provide a systematic assessment of popular DFs in producing activation energies of these representative rhenium-catalyzed organic reactions depicted in Scheme 1. To this end, the high level ab initio coupled cluster method of CCSD(T),[79] which has been shown to be capable of achieving high accuracy for closed-shell TM systems,[80] is employed as the reference in this work.

Unlike many DFT methods, the basis set dependence of ab initio wave function approaches is often more pronounced. To address this point of basis set incompleteness error (BSIE), one procedure often employed is to extrapolate to the complete basis set (CBS) limit by using at least two single point calculations from a series of consecutive basis sets with systematically improved quality. However, for large systems like some in this work, this procedure can be prohibitively expensive in computation. Alternatively, by using explicitly correlated CC approaches, basis set convergence of the traditional ab initio method can be accelerated considerably and as a result electronic correlation energies from a relatively small basis set can be computed close to the CBS limit. Therefore, we herein employed the explicitly correlated coupled cluster CCSD(T)-F12 method as our reference,[81,82] which was obtained also with consideration of the Re 5s5p core−valence correlation.

By comparing our CC reference activation barriers with the DFT results, useful knowledge about DFT performance is gained in this study, which would be helpful to future DFT studies of Re-catalyzed organic transformations. As shown in Scheme 1, the reactions under study contain $C(sp^2)$-H and $C(sp^3)$-H activations, C−C bond formation from activation of unsaturated hydrocarbon, and olefin epoxidation, which represent the typical reactivity catalyzed by rhenium complexes. For computational efficiency consideration of high level CC calculations, we have done some structural simplifications for some reaction systems. Notably, in reaction 2, the original Cp* and Bpin of $Cp^*Re(CO)(R\text{-}H)(Bpin)_2$ complex were truncated to Cp and $B(OH)_2$, respectively. Meanwhile, methane was selected as a model alkane substrate of Re-catalyzed $C(sp^3)$-H activation. For reactions 1 and 2, due to our research interest in C−H activation, we only explored C−H activation processes (reactions 1a and 2a), and the following various reaction elementary steps after C−H activations were not studied in the current work. In reactions 3, we examined not only cycloaddition step (reaction 3a) to generate alkenylrhenium intermediate **3-A** but also the subsequent steps of intramolecular nucleophilic cyclization (reaction 3b) and hydrogen migration (reaction 3c), which separately lead to the different products experimentally observed.

2. COMPUTATIONAL DETAILS

To take the scalar relativistic effects of 5d transition metal Re into account, the new MCDHF relativistic pseudopotential (PP)[83,80e] was applied for Re in all calculations. In our coupled cluster and DFT calculations, we employed correlation consistent basis sets for all atoms,[83,84] and the corresponding PP suffix for Re basis set was omitted hereafter in this paper. For brevity, we used abbreviations for double-ζ, triple-ζ, and quadruple-ζ correlation consistent basis sets as follows, DZ/TZ/QZ for cc-pVDZ/cc-pVTZ/cc-pVQZ and ADZ/ATZ for aug-cc-pVDZ/aug-cc-pVTZ.[83] Because of the good performance of PBE0 in previous calibrations for molecular geometries of 5d TM systems,[72,77,85] all the geometries of minima and transition states were uniformly optimized with this functional coupled with the TZ basis set. Vibrational analyses were performed to verify that the optimized structures are proper transition states or minima.

Coupled Cluster Methods. All the coupled cluster CCSD(T) and CCSD(T)-F12 calculations were carried out with the Molpro2010 package.[86] As an alternative and less expensive way to reduce the BSIE than the traditional CBS limit extrapolation, explicitly correlated coupled cluster method is used in this work.[87] The CCSD(T)-F12 approach used herein employs the CCSD(T)-F12b method with the diagonal fixed amplitude 3C(FIX) Ansatz.[82] There is no direct F12 correction to perturbative triples (T), and triples energy contribution is not scaled by a factor of MP2-F12/MP2 in all the CCSD(T)-F12b calculations. For valence correlated CCSD(T)-F12b calculations, we adopted the ADZ basis set (the nonaugmented basis for all H atoms was used, which was suggested to be sufficient in CCSD(T)-F12 calculation[82a]). Since there is still no F12-optimized correlation consistent basis set for transition metals like Re, we consistently used standard aug-cc-pVnZ basis sets.

To have an estimate of the accuracy of our reference CCSD(T)-F12b/ADZ values for valence-only correlation, we have carried out some additional more costly and accurate calculations on the relatively smaller system of olefin epoxidation (reaction 4 in Scheme 1), which are too expensive to be done for other reactions in Scheme 1. First, we improved the basis set in CCSD(T)-F12b calculation from ADZ to ATZ (for ATZ calculations the nonaugmented basis for all H atoms was used), and using these two basis set, the CCSD(T)-F12b/CBS results were then obtained according to the available Schwenke's two-point CBS limit extrapolation scheme[88] for CCSD(T)-F12b correlation energy shown in eq 1, with CCSD-F12b correlation energy and perturbative triples contribution (T) extrapolated separately. In eq 1, n is the cardinal number of the basis sets (n = 2, 3 for ADZ, ATZ), while the optimal parameter *pow* in CBS limit extrapolation was chosen to be 2.48307 for (R)CCSD-F12b and 2.7903 for perturbative triples (T) contribution, which was determined for ADZ-ATZ extrapolation.[89] The Hartree−Fock (HF) CBS limit in

dx.doi.org/10.1021/ct4010855 | J. Chem. Theory Comput. 2014, 10, 579−588

Table 1. Reaction Barrier Height $\Delta E^{\ddagger}_{val}$ (kcal/mol) from Valence-Only Correlation Calculations Using CCSD(T) and CCSD(T)-F12b Method for Olefin Epoxidation Reaction (Reaction 4 in Scheme 1) at Various Levels

	CCSD(T)-F12b/ADZ	CCSD(T)-F12b/ATZ	CCSD(T)-F12b/CBS(ADZ-ATZ)	CCSD(T)/ADZ	CCSD(T)/ATZ	CCSD(T)/CBS(ADZ-ATZ)
$\Delta E^{\ddagger}_{val}$	19.28	18.96	18.66	14.06	17.77	19.07

CCSD(T)-F12b/CBS value was not obtained from extrapolation but was approximated by the SCF+CABS-singles energy[90] calculated with the ATZ basis set used in CCSD(T)-F12b calculations.

$$E_{corr,n} = E_{corr,CBS} + \frac{A}{n^{pow}} \quad (1)$$

In addition to the test of CCSD(T)-F12b with a larger basis set, we also carried out traditional canonical CCSD(T) calculations with ADZ and ATZ basis sets and obtained CCSD(T)/CBS results thereof by using the two-point CBS limit extrapolation eq 2 for total electronic energy.[91] This extrapolation formula was found recently to be relatively better for CCSD(T) in comparison with several others.[92] The testing results shown in Table 1 indicate that the $\Delta E^{\ddagger}_{val}$ value obtained at the ADZ level (19.28 kcal/mol) is only 0.62 and 0.21 kcal/mol away from the CCSD(T)-F12b/CBS (18.66 kcal/mol) and CCSD(T)/CBS (19.07 kcal/mol) values, indicating an acceptable balance between computational accuracy and cost of the CCSD(T)-F12b/ADZ calculations (Table S1 in the Supporting Information contains the original raw data to generate results in Table 1).

$$E_{total,n} = E_{total,CBS} + \frac{A}{(n+1/2)^4} \quad (2)$$

In both ADZ and ATZ calculations by the CCSD(T)-F12b method, density fitting of the Fock and exchange matrices used the auxiliary basis sets, def2-AQZVPP/JKFIT[93] for Re atom, and aug-cc-pVTZ/JKFIT[94] for the rest of the atoms (all H atoms used cc-pVTZ/JKFIT instead), while density fitting of the other two-electron integrals employed aug-cc-pVTZ-PP/MP2FIT[95] for Re and aug-cc-pVTZ/MP2FIT[96] for the rest of the atoms (all H atoms used cc-pVTZ/MP2FIT instead). Resolution of the identity (RI) approximation utilized a complementary auxiliary basis set (CABS) approach[97] using the same JKFIT auxiliary basis set as used in density fitting.

The Re 5s5p correlation effects in all complexes were considered using the CCSD(T)-F12b method as well. In Re 5s5p core−valence correlation calculations, the correlation consistent weighted core−valence double-ζ basis set cc-pwCVDZ was used for Re,[80e] and for the remaining main group elements (C, O, N, B, Br, H) the DZ basis set[84] was employed. We denote this combination of basis sets as wDZ. Density fitting of the Fock and exchange matrices as well as RI approximation used the auxiliary basis set def2-QZVPP/JKFIT[93] for the Re atom and cc-pVTZ/JKFIT[94] for the rest of the atoms, while density fitting of the other two-electron integrals employed cc-pwCVTZ-PP/MP2FIT[95] for Re and cc-pVTZ/MP2FIT[96] for the rest of the atoms. Consistent with previous computational practices,[75,76,98] the value of the geminal Slater exponent in our valence-only and core−valence correlated CCSD(T)-F12b calculations was chosen to be 1.4 a_0^{-1}

The valence-only correlated ab initio barriers $\Delta E^{\ddagger}_{val}$ from the CCSD(T)-F12b/ADZ level were corrected to produce the final $\Delta E^{\ddagger}_{final}$ data based on eq 3. $\Delta\Delta E^{\ddagger}_{5s5p}$ denotes the Re 5s5p core−valence correlation correction for $\Delta E^{\ddagger}_{val}$, and it was obtained by the difference of two sets of calculations, with and without the corresponding core−valence correlation using the same wDZ basis set. The $\Delta E^{\ddagger}_{final}$ values can serve as our reference for testing the various DFT functionals.

$$\Delta E^{\ddagger}_{final} = \Delta E^{\ddagger}_{val} + \Delta\Delta E^{\ddagger}_{5s5p} \quad (3)$$

Density Functional Methods. All DFT calculations were done using the Gaussian 09 program.[99] We employed 16 DFs which cover the range from GGA, meta-GGA, to hybrid GGA, hybrid meta-GGA, and double-hybrid DFs: PBE0,[100] PBE,[100a] M06,[101] M06-L,[101a] M06-2X,[101] TPSS,[102] TPSSh,[102] B3LYP,[103] B2GP-PLYP,[104] B2-PLYP,[105] ωB97X,[106] OLYP,[103b,107] BMK,[108] BP86,[103a,109] CAM-B3LYP,[110] and LC-ωPBE.[111] In single point calculations with double-hybrid DFs, the core electrons of non-hydrogen atoms were correlated in the MP2-type correlation treatment. A test of barrier heights obtained with B3LYP/TZ for all the reactions showed a maximum difference of 0.12 kcal/mol compared with the B3LYP/QZ results (see Table S2 in the Supporting Information), hence indicating that the TZ basis set already gives values close to convergence for DFT. Therefore, DFT barrier height calculations using 16 DFs were all done in conjunction with the TZ basis set for all the reactions in Scheme 1. In addition, we tested the effect of dispersion correction using Grimme's DFT-D3 method with zero short-range damping denoted as DFT-D3(0).[112,113] There are no DFT-D3(0) parameters for the ωB97X functional, thus the empirical dispersion corrected functional ωB97XD designed by its original developers was used instead.[114]

3. RESULTS AND DISCUSSION

Table 2 summarizes valence correlated activation energies $\Delta E^{\ddagger}_{val}$ and Re 5s5p core−valence correlation correction $\Delta\Delta E^{\ddagger}_{5s5p}$

Table 2. CCSD(T)-F12b Calculated Reaction Barriers $\Delta E^{\ddagger}_{val}$ and Re 5s5p Correlation Corrections $\Delta\Delta E^{\ddagger}_{5s5p}$ of All the Reactions (kcal/mol)

reaction	1a	2a	3a	3b	3c	4
$\Delta E^{\ddagger}_{val}$[a]	24.77	11.48	36.87	16.82	21.06	19.28
$\Delta\Delta E^{\ddagger}_{5s5p}$[b]	−0.54	−0.13	0.27	0.21	−0.12	0.12
$\Delta E^{\ddagger}_{final}$[c]	24.23	11.35	37.14	17.03	20.94	19.40

[a]Activation energy is calculated at the valence correlated CCSD(T)-F12b/ADZ level. [b]Re 5s5p core−valence correlation correction $\Delta\Delta E^{\ddagger}_{5s5p}$ is calculated at the CCSD(T)-F12b/wDZ level. [c]$\Delta E^{\ddagger}_{final} = \Delta E^{\ddagger}_{val} + \Delta\Delta E^{\ddagger}_{5s5p}$.

results from the CCSD(T)-F12b method. Being within 0.6 kcal/mol in magnitude, $\Delta\Delta E^{\ddagger}_{5s5p}$ values are very small compared with $\Delta E^{\ddagger}_{val}$. Such generally small magnitudes of 5s5p core−valence correlation are in contrast to the usually sizable magnitudes of 4s4p and 5s5p core−valence correlation up to 1−2 kcal/mol found previously for Zr, Ru and Ir, Pt.[75,76,115] By combining $\Delta E^{\ddagger}_{val}$ and $\Delta\Delta E^{\ddagger}_{5s5p}$ according to eq 3, we obtained the $\Delta E^{\ddagger}_{final}$ as reference values.

Having the reference coupled cluster values $\Delta E^{\ddagger}_{final}$ in hand, we can now assess the performance of DFT methods on all the

dx.doi.org/10.1021/ct4010855 | J. Chem. Theory Comput. 2014, 10, 579−588

Table 3. Various DFT/TZ Calculated MUDs and MSDs of the Reaction Activation Energies $\Delta E^{\ddagger}$ (kcal/mol) without DFT Dispersion Corrections Taking $\Delta E^{\ddagger}_{final}$ as Reference[a]

DF	$\Delta E^{\ddagger}$(1a)	$\Delta E^{\ddagger}$(2a)	$\Delta E^{\ddagger}$(3a)	$\Delta E^{\ddagger}$(3b)	$\Delta E^{\ddagger}$(3c)	$\Delta E^{\ddagger}$(4)	MUD[b]	MSD[b]	MUD[c]	MSD[c]
PBE	−0.90	−2.73	−3.29	−2.30	−5.73	−6.97	3.65	−3.65	2.99	−2.99
PBE0	0.64	−1.06	−0.17	−0.95	−2.51	3.81	1.52	−0.04	1.07	−0.81
LC-ωPBE	−0.86	0.08	4.60	2.92	−0.15	15.05	3.94	3.61	1.72	1.32
B3LYP	3.77	1.86	−0.93	−0.07	−0.49	1.43	1.42	0.93	1.42	0.83
CAM-B3LYP	2.57	2.21	1.38	1.54	1.21	7.20	2.68	2.68	1.78	1.78
OLYP	2.24	−2.40	0.16	−1.49	−6.28	1.95	2.42	−0.97	2.51	−1.55
M06	2.14	0.55	−1.96	−3.06	−1.66	2.50	1.98	−0.25	1.87	−0.80
M06-2X	5.64	1.93	−1.37	−3.34	1.47	10.50	4.04	2.47	2.75	0.87
M06-L	5.97	1.83	−3.46	−5.45	−3.88	−4.52	4.18	−1.59	4.12	−1.00
BMK	2.40	3.63	1.55	0.70	−0.31	7.01	2.60	2.50	1.72	1.59
BP86	−0.60	−2.07	−3.56	−1.77	−5.11	−7.41	3.42	−3.42	2.62	−2.62
TPSS	−0.20	−0.16	−1.75	−1.16	−4.51	−6.84	2.44	−2.44	1.56	−1.56
TPSSh	0.42	0.33	−0.62	−0.73	−3.30	−2.43	1.30	−1.06	1.08	−0.78
ωB97X	2.20	1.40	1.90	0.78	1.37	11.08	3.12	3.12	1.53	1.53
B2-PLYP	6.89	0.00	−0.41	−0.90	−1.96	−3.45	2.27	0.03	2.03	0.72
B2GP-PLYP	−0.34	−0.39	0.62	−0.89	−1.77	−1.51	0.92	−0.71	0.80	−0.55

[a]The labels in parentheses after $\Delta E^{\ddagger}$ denote the corresponding reaction number in Scheme 1. [b]MUD and MSD of $\Delta E^{\ddagger}$ including reaction 4 in Scheme 1. [c]MUD and MSD of $\Delta E^{\ddagger}$ excluding reaction 4 in Scheme 1.

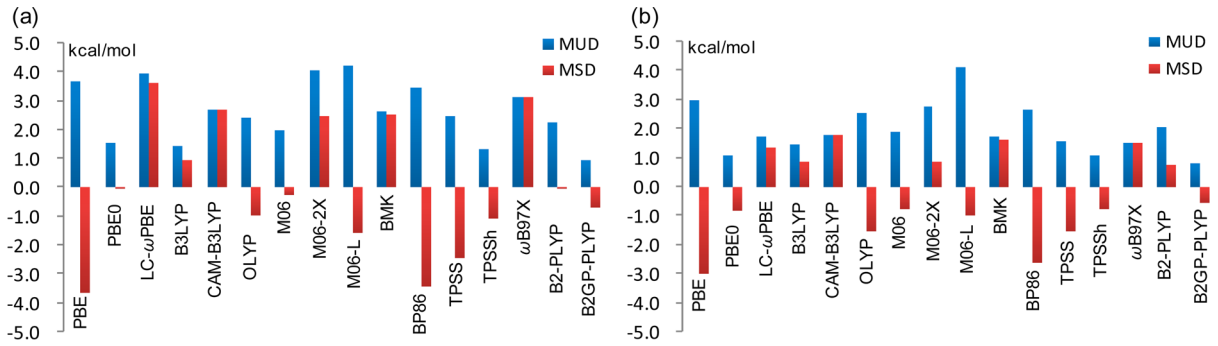

Figure 1. MUDs and MSDs of calculated reaction barriers at the various DFT/TZ levels without DFT dispersion correction, (a) including and (b) excluding reaction 4 in Scheme 1, taking $\Delta E^{\ddagger}_{final}$ as reference.

reaction barriers in Table 2. Using $\Delta E^{\ddagger}_{final}$ value as a reference, the statistical analyses of the mean signed deviation (MSD) and mean unsigned deviation (MUD) of various DFT methods are summarized in Table 3 and depicted in Figure 1 (the DFT data of each reaction were collected in Table S3 in the Supporting Information).

As shown in Table 3 and Figure 1a, there are five DFs with MUDs below 2.0 kcal/mol. The five DFs in the order of increasing MUD are B2GP-PLYP < TPSSh < B3LYP < PBE0 < M06. Of note is that these good DFs are all hybrid or double hybrid ones, and no pure GGA or meta-GGA functionals work better than them. Among all tested DFs, the double hybrid functional B2GP-PLYP, which was shown to perform best in Au-catalyzed reactions and Pt/Ir-promoted C−H activation reactions,[73] produces the smallest MUD of 0.92 kcal/mol and a very small MSD of −0.71 kcal/mol here. In addition, its absolute maximum deviation (MaxD) value of 1.77 kcal/mol is also the smallest among all DFs. So if balanced good performance of all the reaction systems is required, clearly B2GP-PLYP is the most accurate method among these well performing DFs. The MUDs of the other three DFs of TPSSh, B3LYP, and PBE0 are also quite small (<1.6 kcal/mol), which indicates they are good choices if a less computationally expensive hybrid DF than the double hybrid DF is preferred. Interestingly, though B3LYP, TPSSh, and PBE0 have similarly small MUDs, they show different patterns of performance on a specific reaction. B3LYP have a comparatively larger deviation for the C(sp^2)-H activation reaction (reaction 1a), while TPSSh and PBE0 perform relatively worse on the other two reactions (reactions 3c and 4). Concerning the direction of the deviations, we note that two range-separated functionals CAM-B3LYP and ωB97X consistently overestimate the activation energies of all the reactions, while the opposite is true for pure functional PBE, BP86, and TPSS.

It is noteworthy that the olefin epoxidation reaction (Table 2, reaction 4) catalyzed by a high-valent organorhenium(VII) bisperoxo complex is quite different compared with other reactions involving only a low-valent rhenium(I)/(III) formal oxidation state, since many tested DFs (PBE, M06-2X, CAM-B3LYP, BMK, BP86, TPSS, ωB97X, LC-ωPBE) perform very poorly to have large deviations (from 6 to 15 kcal/mol) for reaction 4, and only three DFs of B3LYP, B2GP-PLYP, and OLYP perform well with deviations smaller than 2 kcal/mol. Hence, we also investigated the results of MUD/MSD excluding reaction 4. The statistical analyses thereof collected in Table 3 and Figure 1b show that, by leaving out the reaction 4, almost all DFs improve their performances with only one exception of OLYP, and DFs with MUDs below 2.0 kcal/mol include five additional ones of ωB97X, TPSS, LC-ωPBE, BMK, and CAM-B3LYP. In general, the hybrid DFs like PBE0,

dx.doi.org/10.1021/ct4010855 | J. Chem. Theory Comput. 2014, 10, 579−588

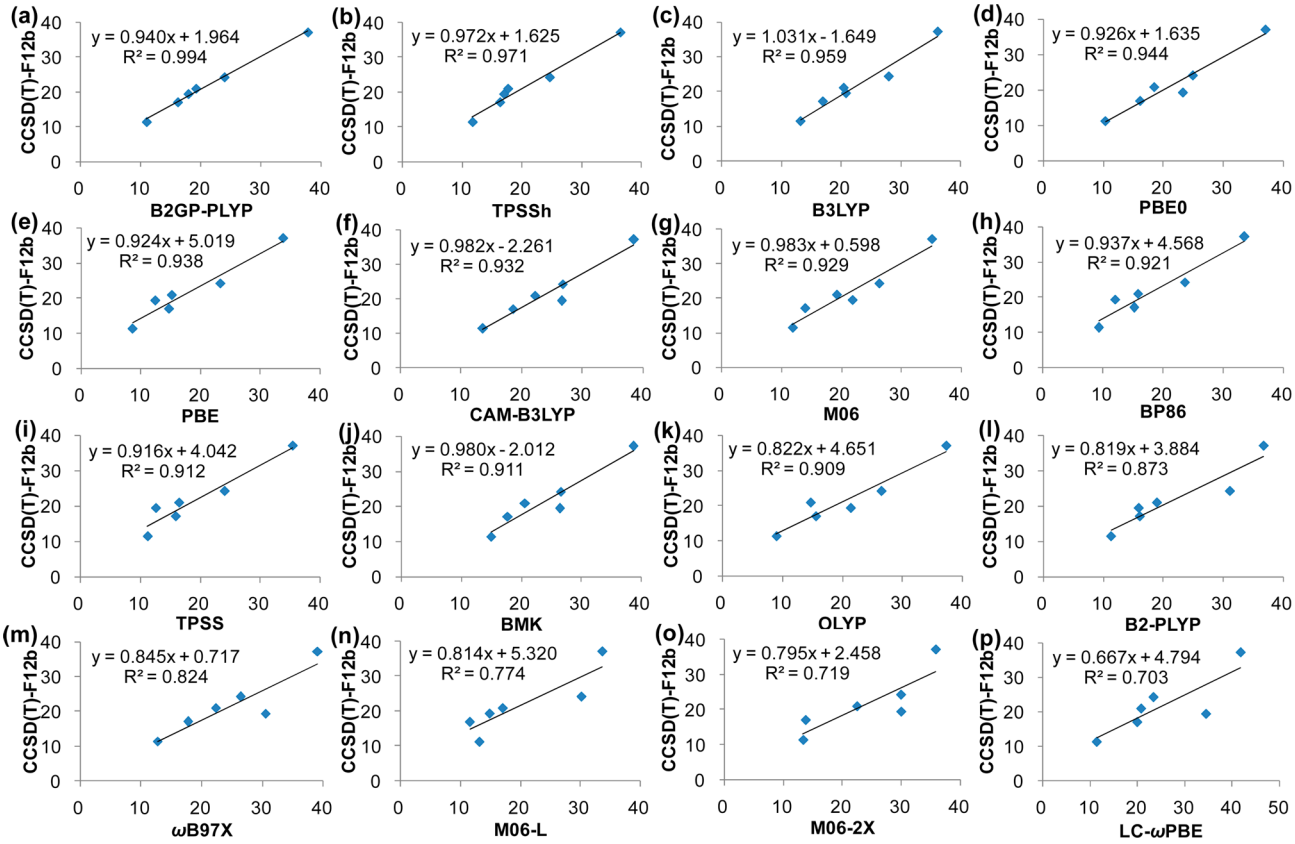

Figure 2. Correlations of calculated barriers (kcal/mol) for all the reactions in Scheme 1 between reference $\Delta E^{\ddagger}_{final}$ and various DFT values without DFT dispersion corrections.

Table 4. Various DFT/TZ Calculated MUDs and MSDs of the Activation Energies (kcal/mol) with DFT Dispersion Corrections, Taking $\Delta E^{\ddagger}_{final}$ as Reference (kcal/mol)[a]

DF	$\Delta E^{\ddagger}$(1a)	$\Delta E^{\ddagger}$(2)	$\Delta E^{\ddagger}$(3a)	$\Delta E^{\ddagger}$(3b)	$\Delta E^{\ddagger}$(3c)	$\Delta E^{\ddagger}$(4)	MUD[b]	MSD[b]	MUD[c]	MSD[c]
PBE	−0.67	−3.08	−4.57	−3.41	−5.56	−8.63	4.32	−4.32	3.46	−3.46
PBE0	0.90	−1.38	−1.50	−2.21	−2.29	1.90	1.70	−0.76	1.66	−1.30
LC-ωPBE	−0.56	−0.28	1.96	1.27	0.18	12.58	2.97	2.69	1.05	0.71
B3LYP	4.16	1.29	−3.22	−2.35	−0.09	−1.93	2.17	−0.36	2.22	−0.04
CAM-B3LYP	2.84	1.88	−0.17	−0.01	1.53	4.87	1.88	1.82	1.29	1.21
OLYP	3.08	−2.80	−5.25	−4.01	−5.05	−5.73	4.32	−3.29	4.04	−2.81
M06	2.25	0.58	−2.01	−3.05	−1.64	2.50	2.00	−0.23	1.90	−0.78
M06-2X	5.66	1.95	−1.41	−3.33	1.49	10.50	4.06	2.48	2.77	0.87
M06-L	6.00	1.85	−3.51	−5.44	−3.86	−4.52	4.20	−1.58	4.13	−0.99
BMK	2.75	3.01	−0.96	−2.06	0.20	3.08	2.01	1.01	1.80	0.59
BP86	−0.27	−2.75	−6.28	−4.27	−4.69	−11.13	4.90	−4.90	3.65	−3.65
TPSS	0.06	−0.66	−3.67	−2.86	−4.25	−9.37	3.48	−3.46	2.30	−2.27
TPSSh	0.73	−0.16	−2.45	−2.46	−3.02	−4.99	2.30	−2.06	1.76	−1.47
ωB97X	1.96	0.40	−0.04	−0.57	0.20	7.91	1.85	1.64	0.63	0.39
B2-PLYP	7.09	−0.27	−1.67	−2.20	−1.69	−5.36	3.05	−0.68	2.58	0.25
B2GP-PLYP	−0.20	−0.59	−0.29	−1.86	−1.58	−2.90	1.24	−1.24	0.90	−0.90

[a]The labels in parentheses after $\Delta E^{\ddagger}$ denote the corresponding reaction number in Scheme 1. [b]MUD and MSD of $\Delta E^{\ddagger}$ including reaction 4 in Scheme 1. [c]MUD and MSD of $\Delta E^{\ddagger}$ excluding reaction 4 in Scheme 1.

TPSSh, and M06 with a medium percentage of HF exchange (10−27%) still tend to perform better to produce smaller MUDs than the corresponding pure DFs PBE, TPSS, and M06-L without any HF exchange.

In the above considerations, we evaluate the DFT performance in terms of barrier heights. Often more important in the reaction mechanism studies is the trend discovery. To investigate this aspect of DFT performance, we separately plotted 16 correlations between $\Delta E^{\ddagger}_{final}$ and those barriers from the various DFs in Figure 2. One can see that the correlations ($R^2 > 0.94$) for the four overall best-performing DFs (B2GP-PLYP, TPSSh, B3LYP, PBE0) are the same as the four ones having the smallest MUDs, which indicates that the barrier trend performance and the barrier height performance of DFs are in accord, as found before in reaction barrier calculations involving Au, Rh, Pd, Ir, and Pt.[73,74] The slope of the

dx.doi.org/10.1021/ct4010855 | J. Chem. Theory Comput. 2014, 10, 579−588

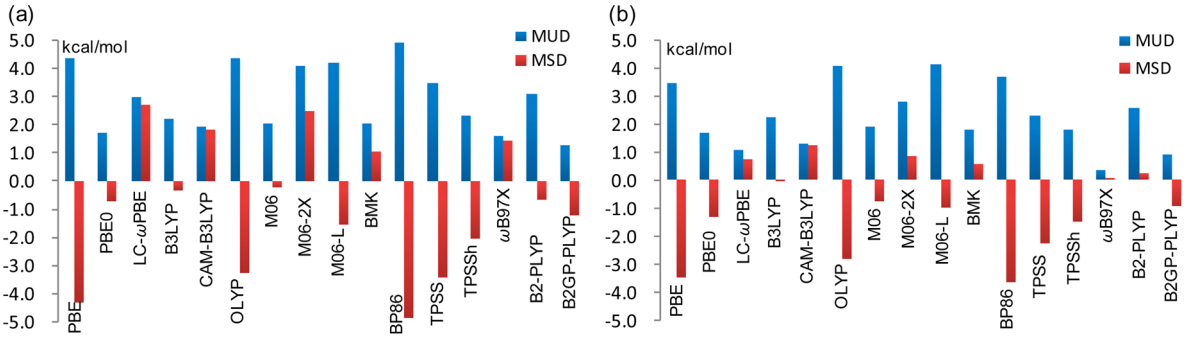

Figure 3. MUDs and MSDs of calculated reaction barriers at the various DFT/TZ levels with DFT dispersion correction (a) including and (b) excluding reaction 4, taking $\Delta E^{\ddagger}_{final}$ as reference.

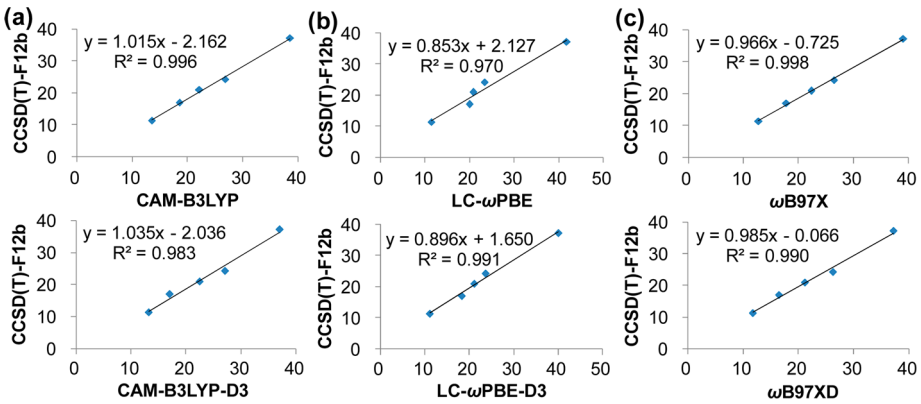

Figure 4. Correlations between $\Delta E^{\ddagger}_{final}$ and DFT-calculated barriers (kcal/mol) from (a) CAM-B3LYP and CAM-B3LYP-D3, (b) LC-ωPBE and LC-ωPBE-D3, (c) ωB97X and ωB97XD, all in the absence of reaction 4.

correlation line can be used to quantitatively describe the reactivity difference and trend, which is reflected by the error in relative reaction barriers between different reactions, and the intercept of the correlation line can be employed to judge the systematic barrier underestimation/overestimation of a DFT method. As shown in Figure 2, the B2GP-PLYP functional that gives the smallest MUD and MaxD in performance assessment about barrier heights here affords the comparatively worse slope and intercept values than the TPSSh and B3LYP functionals in this regard. The slope and intercept of the correlation lines of TPSSh and B3LYP are quite close to the ideal 1.0 (deviation within 0.031 from 1.0) and to the ideal zero (deviation within 1.65 kcal/mol from zero), respectively. Both points indicate that for B3LYP and TPSSh barrier trends are well followed and systematic underestimation/overestimation of barriers by the DFs are small. It should be mentioned that LC-ωPBE, M06-L, and M06-2X have the worst three assessment parameters (R^2, slope, and intercept), which is in line with their poorest performance in barrier height calculations as shown in Table 3. The result implies that these three functionals should be avoided for Re-catalyzed reactions without empirical dispersion correction.

Finally, concerning the empirical dispersion correction for DFT, we summarized the corresponding results in Table 4 and Figure 3. Comparing Table 3 and 4, for all reactions 1−4 we note that the empirical dispersion corrections only reduced the MUDs of four DFs, i.e. ωB97X, BMK, LC-ωPBE and CAM-B3LYP, by 0.6−1.3 kcal/mol. For the majority of DFs, including the well performed B2GP-PLYP, TPSSh, B3LYP, and PBE0, DFT-D3(0) corrections turn out to slightly spoil an already good performance. As found before,[72−76] the results of the M06 series DFs are almost not affected by adding dispersion corrections, due to the way of their parametrization to account for dispersion interaction to a certain extent.[101] In terms of MUDs below 2.0 kcal/mol, here we find the best four DFs are B2GP-PLYP, PBE0, ωB97X, and CAM-B3LYP, with the MUDs of 1.24, 1.70, 1.85, 1.88 kcal/mol, respectively. The DFs with MUDs larger than 2.0 kcal/mol but still smaller than 2.5 kcal/mol include M06, BMK, B3LYP, and TPSSh (in the MUD-increasing order). It should be noted that more bulky reaction systems than the reaction models under study may bring larger dispersion corrections.

For the organorhenium(VII) bisperoxo-catalyzed reaction 4, DFT dispersion corrections reduce the absolute deviations of only five DFs, i.e., PBE0, ωB97X, CAM-B3LYP, LC-ωPBE, and BMK, by about 2−4 kcal/mol. In fact, after adding the dispersion correction, the deviation of reaction 4 from some of these DFs is still as large as about 12 kcal/mol. Under such circumstances, the MUD/MSD results excluding reaction 4 were examined (shown in Table 4 and Figure 3b). It can be seen from Table 4 and Figure 3b that similar to the case without dispersion correction, by leaving out reaction 4, the MUDs of almost all DFs are reduced to various extents, with the exception of B3LYP, whose MUD is slightly larger than that with reaction 4. Concerning the effect of DFT dispersion correction, when leaving out reaction 4, the use of DFT empirical dispersion corrections leads to better agreement with benchmark values only for three range-separated DFs, i.e., ωB97X, CAM-B3LYP, and LC-ωPBE. Especially for ωB97XD, DFT dispersion correction reduces its MUD to the smallest 0.63 kcal/mol among all tested DFs in the absence of reaction 4. Thus for barrier height calculations of reactions catalyzed by

dx.doi.org/10.1021/ct4010855 | J. Chem. Theory Comput. 2014, 10, 579−588

rhenium(I)/(III) carbonyl complexes, ωB97XD definitely performs best among all the tested DFs.

Because for the majority of tested DFs, DFT-D3(0) corrections lead to larger deviations from the benchmark values, here we shall not further discuss the correlations of DFT barriers with reference $\Delta E^{\ddagger}_{final}$ data after adding the DFT dispersion corrections and relegate them into the Supporting Information (see Figure S1 for details). Notwithstanding, in the absence of reaction 4, DFT dispersion corrections reduced the MUD of three range-separated DFs of ωB97X, CAM-B3LYP, and LC-ωPBE to difference extents as shown in Table 4. Hence we plotted the barriers from these three DFs excluding reaction 4 with and without DFT dispersion corrections in Figure 4. Although the MUD and MSD for CAM-B3LYP and LC-ωPBE are improved after adding DFT-D3(0) dispersion corrections, the correlation R^2, the slope, and the intercept of the correlation line for this DF are almost not improved. However, along with its decreased MUD and MSD, ωB97XD notably gets two of these three assessment parameters (R^2, slope, and intercept) improved in comparison with ωB97X. This can be seen from the facts that the slope of the correlation line are extremely close to the ideal 1.0 (deviation of 0.015), and the intercept value (0.066) is also extremely close to the ideal zero. In view of this best barrier trend performance as well as the best barrier height performance (MUD), ωB97XD is definitely recommended from all the well-performing DFs for both barrier height calculations and barrier trend studies of reactions catalyzed by rhenium(I)/(III) carbonyl complexes. Coincidentally and interestingly, the ωB97XD was also found recently by Chan and Ball to render good performances for the geometry optimization as well as the binding energy for Re-alkane complexes.[59] In our opinion, it represents a reliable and cost-efficient means to study rhenium(I)/(III) carbonyl complex-mediated reactions. If reaction 4 is in the testing set and more balanced performance is required, PBE0-D3 can be recommended since it bears the smallest MaxD (about 2.3 kcal/mol) among all tested DFs with DFT dispersion corrections.

4. CONCLUSIONS

We herein have systematically assessed the performances of commonly used DFT methods (PBE, TPSS, B3LYP, CAM-B3LYP, OLYP, PBE0, LC-ωPBE, M06, M06-2X, M06-L, BP86, BMK, ωB97X, TPSSh, B2-PLYP, and B2GP-PLYP) for barrier heights and barrier trends of some typical Re-catalyzed reactions. By employing the high level explicitly correlated CCSD(T)-F12 method, our reference ab initio coupled cluster calculations address both the valence correlation BSIE issue and the Re 5s5p core−valence correlation effect. The reactions under study include those catalyzed by both low-valent rhenium(I)/(III) carbonyl complexes and a high-valent organorhenium(VII) bisperoxo complex.

For all the tested reactions including C−H activations, C−C formation, and C═C epoxidation, without DFT empirical dispersion corrections, we found that the four best-performing DFs for the barrier heights are B2GP-PLYP, TPSSh, B3LYP, and PBE0, all with MUDs under 1.6 kcal/mol. Among these four DFs, B2GP-PLYP generates more accurate barrier heights, while B3LYP and TPSSh are more suitable for barrier trend study for these Re-catalyzed reactions. In general, the pure DFs of TPSS, BP86, OLYP, PBE, and M06-L are found to perform uniformly worse than many hybrid and double hybrid ones like B2GP-PLYP, TPSSh, B3LYP, PBE0, and M06. DFT empirical dispersion corrections have detrimental or no effect on MUDs except for BMK, CAM-B3LYP, LC-ωPBE, and ωB97X, for which certain improvements up to about 1.3 kcal/mol on MUD are observed.

Of note is that reactions involving high-valent organorhenium(VII) bisperoxo complex and low-valent rhenium(I)/(III) carbonyl complexes are quite different, because the former is associated with very large errors up to about 15 kcal/mol in barrier height calculations with many DFs, except only few ones having errors smaller than 2 kcal/mol, like B3LYP, B2GP-PLYP, and OLYP. Despite the fact that DFT dispersion correction can improve somewhat the results of this high-valent organorhenium(VII) reaction for five DFs, namely, BMK, CAM-B3LYP, ωB97X, LC-ωPBE, and PBE0, it does not largely solve this large error problem.

For reactions involving only low-valent rhenium(I)/(III) carbonyl complexes, the empirical dispersion corrected ωB97XD perform quite well. Its impressive small MUD of about 0.6 kcal/mol apparently outperforms other DFs, which we strongly recommend for both the barrier height and the barrier trend studies of reactions catalyzed or mediated by rhenium(I)/(III) carbonyl complexes.

■ ASSOCIATED CONTENT

Ⓢ Supporting Information

Four tables and one figure of computational results and Cartesian coordinates of all species. This material is available free of charge via the Internet at http://pubs.acs.org.

■ AUTHOR INFORMATION

Corresponding Author

*E-mail: chenh@iccas.ac.cn.

Notes

The authors declare no competing financial interest.

■ ACKNOWLEDGMENTS

This work was supported by the National Natural Science Foundation of China (NSFC, Grants 21290194 and 21221002) and the Institute of Chemistry, Chinese Academy of Sciences.

■ REFERENCES

(1) (a) Kuninobu, Y.; Takai, K. *Chem. Rev.* **2011**, *111*, 1938−1953. (b) Hua, R.; Jiang, J.-L. *Curr. Org. Synth.* **2007**, *4*, 151−174.

(2) (a) Boag, N. M.; Kaesz, H. D. *Comprehensive Organometallic Chemistry*; Wilkinson, G., Stone, F. G. A., Abel, E. W., Eds.; Pergamon Press: Oxford, U.K., 1982; Vol. *4*, pp 161−242. (b) O'Connor, J. M. *Comprehensive Organometallic Chemistry II*; Abel, E. W., Stone, F. G. A., Wilkinson, G., Eds.; Pergamon Press: Oxford, U.K., 1995; Vol. *6*, pp 167−229. (c) Hoffman, D. M. *Comprehensive Organometallic Chemistry II*; Abel, E. W., Stone, F. G. A., Wilkinson, G., Eds.; Pergamon Press: Oxford, U.K., 1995; Vol. *6*, pp 231−255. (d) Romao, C. C.; Royo, B. *Comprehensive Organometallic Chemistry III*; Crabtree, R. H., Mingos, D. M. P., Eds.; Elsevier: Amsterdam, The Netherlands, 2007; Vol. *5*, pp 855−960.

(3) Kuninobu, Y.; Kawata, A.; Takai, K. *J. Am. Chem. Soc.* **2005**, *127*, 13498−13499.

(4) Kuninobu, Y.; Tokunaga, Y.; Kawata, A.; Takai, K. *J. Am. Chem. Soc.* **2006**, *128*, 202−209.

(5) Kuninobu, Y.; Nishina, Y.; Nakagawa, C.; Takai, K. *J. Am. Chem. Soc.* **2006**, *128*, 12376−12377.

(6) (a) Kuninobu, Y.; Nishina, Y.; Shouho, M.; Takai, K. *Angew. Chem., Int. Ed.* **2006**, *45*, 2766−2768. (b) Kuninobu, Y.; Nishina, Y.; Takai, K. *Org. Lett.* **2006**, *8*, 2891−2893.

(7) (a) Tang, Q.; Xia, D.; Jin, X.; Zhang, Q.; Sun, X. Q.; Wang, C. *J. Am. Chem. Soc.* **2013**, *135*, 4628−4631. (b) Xia, D.; Wang, Y.; Du, Z.; Zheng, Q. Y.; Wang, C. *Org. Lett.* **2012**, *14*, 588−591.
(8) Chen, H.; Hartwig, J. F. *Angew. Chem., Int. Ed.* **1999**, *38*, 3391−3393.
(9) Kuninobu, Y.; Kawata, A.; Nishi, M.; Yudha, S. S.; Chen, J.-j.; Takai, K. *Chem. Asian J.* **2009**, *4*, 1424−1433.
(10) Kuninobu, Y.; Kawata, A.; Takai, K. *Org. Lett.* **2005**, *7*, 4823−4825.
(11) (a) Kühn, F. E.; Herrmann, W. A. *Struct. Bonding (Berlin)* **2000**, *97*, 213−236. (b) Kühn, F. E.; Scherbaum, A.; Herrmann, W. A. *J. Organomet. Chem.* **2004**, *689*, 4149−4164. (c) Kühn, F. E.; Santos, A. M.; Herrmann, W. A. *Dalton Trans.* **2005**, 2483−2491.
(12) Herrmann, W. A.; Fischer, R. W.; Scherer, W.; Rauch, M. U. *Angew. Chem., Int. Ed. Engl.* **1993**, *32*, 1157−1160.
(13) Di Valentin, C.; Gandolfi, R.; Gisdakis, P.; Rösch, N. *J. Am. Chem. Soc.* **2001**, *123*, 2365−2376.
(14) Gisdakis, P.; Yudanov, I. V.; Rösch, N. *Inorg. Chem.* **2001**, *40*, 3755−3765.
(15) Rotzinger, F. P. *Chem. Rev.* **2005**, *105*, 2003−2037.
(16) Niu, S.; Hall, M. B. *Chem. Rev.* **2000**, *100*, 353−405.
(17) Balcells, D.; Clot, E.; Eisenstein, O. *Chem. Rev.* **2010**, *110*, 749−823.
(18) Siegbahn, P. E. M.; Blomberg, M. R. A. *Chem. Rev.* **2000**, *100*, 421−437.
(19) Noodleman, L.; Lovell, T.; Han, W.-G.; Li, J.; Himo, F. *Chem. Rev.* **2004**, *104*, 459−508.
(20) Baik, M.-H.; Newcomb, M.; Friesner, R. A.; Lippard, S. J. *Chem. Rev.* **2003**, *103*, 2385−2419.
(21) Shaik, S.; Cohen, S.; Wang, Y.; Chen, H.; Kumar, D.; Thiel, W. *Chem. Rev.* **2010**, *110*, 949−1017.
(22) Cramer, C. J.; Truhlar, D. G. *Phys. Chem. Chem. Phys.* **2009**, *11*, 10757−10816.
(23) Ziegler, T.; Autschbach, J. *Chem. Rev.* **2005**, *105*, 2695−2722.
(24) Torrent, M.; Solà, M.; Frenking, G. *Chem. Rev.* **2000**, *100*, 439−493.
(25) Dedieu, A. *Chem. Rev.* **2000**, *100*, 543−600.
(26) de Jong, G. T.; Bickelhaupt, F. M. *J. Chem. Theory Comput.* **2006**, *2*, 322−335.
(27) Swart, M. *J. Chem. Theory Comput.* **2008**, *4*, 2057−2066.
(28) Quintal, M. M.; Karton, A.; Iron, M. A.; Boese, A. D.; Martin, J. M. L. *J. Phys. Chem. A* **2006**, *110*, 709−716.
(29) Seth, M.; Ziegler, T.; Steinmetz, M.; Grimme, S. *J. Chem. Theory Comput.* **2013**, *9*, 2286−2299.
(30) Kazaryan, A.; Baerends, E. J. *J. Comput. Chem.* **2013**, *34*, 870−878.
(31) Fang, Z. T.; Dixon, D. A. *J. Phys. Chem. C* **2013**, *117*, 7459−7474.
(32) Moncho, S.; Brothers, E. N.; Janesko, B. G. *J. Phys. Chem. C* **2013**, *117*, 7487−7496.
(33) Sniatynsky, R.; Janesko, B. G.; El-Mellouhi, F.; Brothers, E. N. *J. Phys. Chem. C* **2012**, *116*, 26396−26404.
(34) Fang, Z. T.; Outlaw, M. D.; Smith, K. K.; Gist, N. W.; Li, S. G.; Dixon, D. A. *J. Phys. Chem. C* **2012**, *116*, 8475−8492.
(35) Sun, X. L.; Huang, X. R.; Li, J. L.; Huo, R. P.; Sun, C. C. *J. Phys. Chem. A* **2012**, *116*, 1475−1485.
(36) Oyedepo, G. A.; Wilson, A. K. *ChemPhysChem* **2011**, *12*, 3320−3330.
(37) Li, S. G.; Guenther, C. L.; Kelley, M. S.; Dixon, D. A. *J. Phys. Chem. C* **2011**, *115*, 8072−8103.
(38) Wang, T.-H.; Fang, Z. T.; Gist, N. W.; Li, S. G.; Dixon, D. A. *J. Phys. Chem. C* **2011**, *115*, 9344−9360.
(39) Anoop, A.; Thiel, W.; Neese, F. *J. Chem. Theory Comput.* **2010**, *6*, 3137−3144.
(40) Jiménez-Hoyos, C. A.; Janesko, B. G.; Scuseria, G. E. *J. Phys. Chem. A* **2009**, *113*, 11742−11749.
(41) Handzlik, J. *Chem. Phys. Lett.* **2009**, *469*, 140−144.
(42) Piacenza, M.; Hyla-Kryspin, I.; Grimme, S. *J. Comput. Chem.* **2007**, *28*, 2275−2285.
(43) de Jong, G. T.; Geerke, D. P.; Diefenbach, A.; Solà, M.; Bickelhaupt, F. M. *J. Comput. Chem.* **2005**, *26*, 1006−1020.
(44) de Jong, G. T.; Geerke, D. P.; Diefenbach, A.; Bickelhaupt, F. M. *Chem. Phys.* **2005**, *313*, 261−270.
(45) Li, H. X.; Lu, G.; Jiang, J. L.; Huang, F.; Wang, Z. X. *Organometallics* **2011**, *30*, 2349−2363.
(46) Hölscher, M.; Leitner, W.; Holthausen, M. C.; Frenking, G. *Chem.—Eur. J.* **2005**, *11*, 4700−4708.
(47) Schultz, N. E.; Gherman, B. F.; Cramer, C. J.; Truhlar, D. G. *J. Phys. Chem. B* **2006**, *110*, 24030−24046.
(48) Nava, P.; Hagebaum-Reignier, D.; Humbel, S. *ChemPhysChem* **2012**, *13*, 2090−2096.
(49) Faza, O. N.; Rodríguez, R. Á.; López, C. S. *Theor. Chem. Acc.* **2011**, *128*, 647−661.
(50) Li, S. G.; Zhai, H. J.; Wang, L. S.; Dixon, D. A. *J. Phys. Chem. A* **2012**, *116*, 5256−5271.
(51) Li, S. G.; Dixon, D. A. *J. Phys. Chem. C* **2011**, *115*, 19190−19196.
(52) Li, S. G.; Dixon, D. A. *J. Phys. Chem. A* **2010**, *114*, 2665−2683.
(53) Li, S. G.; Dixon, D. A. *J. Phys. Chem. A* **2008**, *112*, 6646−6666.
(54) Chen, M. Y.; Dixon, D. A. *J. Phys. Chem. A* **2013**, *117*, 3676−3688.
(55) Lawson Daku, L. M.; Aquilante, F.; Robinson, T. W.; Hauser, A. *J. Chem. Theory Comput.* **2012**, *8*, 4216−4231.
(56) Li, S. G.; Zhai, H. J.; Wang, L. S.; Dixon, D. A. *J. Phys. Chem. A* **2009**, *113*, 11273−11288.
(57) Shi, Y.-K.; Li, Z. H.; Fan, K.-N. *J. Phys. Chem. A* **2010**, *114*, 10297−10380.
(58) Harvey, J. N.; Aschi, M. *Faraday Discuss.* **2003**, *124*, 129−143.
(59) Chan, B.; Ball, G. E. *J. Chem. Theory Comput.* **2013**, *9*, 2199−2208.
(60) Chan, B.; Yim, W.-L. *J. Chem. Theory Comput.* **2013**, *9*, 1964−1970.
(61) Chen, M. Y.; Craciun, R.; Hoffman, N.; Dixon, D. A. *Inorg. Chem.* **2012**, *51*, 13195−13203.
(62) Fang, H.-C.; Li, Z. H.; Fan, K.-N. *Phys. Chem. Chem. Phys.* **2011**, *13*, 13358−13369.
(63) Averkiev, B. B.; Zhao, Y.; Truhlar, D. G. *J. Mol. Catal. A: Chem.* **2010**, *324*, 80−88.
(64) Varganov, S. A.; Olson, R. M.; Gordon, M. S. *J. Chem. Phys.* **2004**, *120*, 5169−5175.
(65) Li, S. G.; Hennigan, J. M.; Dixon, D. A.; Peterson, K. A. *J. Phys. Chem. A* **2009**, *113*, 7861−7877.
(66) Shirley, R.; Liu, Y. Y.; Totton, T. S.; West, R. H.; Kraft, M. *J. Phys. Chem. A* **2009**, *113*, 13790−13796.
(67) Pratt, L. M.; Voit, S.; Mai, B. K.; Nguyen, B. H. *J. Phys. Chem. A* **2010**, *114*, 5005−5015.
(68) Pratt, L. M.; Voit, S.; Okeke, F. N. *J. Phys. Chem. A* **2011**, *115*, 2281−2290.
(69) Chen, H.; Cho, K.-B.; Lai, W. Z.; Nam, W.; Shaik, S. *J. Chem. Theory Comput.* **2012**, *8*, 915−926.
(70) Chen, H.; Lai, W. Z.; Yao, J. N.; Shaik, S. *J. Chem. Theory Comput.* **2011**, *7*, 3049−3053.
(71) Chen, H.; Lai, W. Z.; Shaik, S. *J. Phys. Chem. Lett.* **2010**, *1*, 1533−1540.
(72) Kang, R. H.; Chen, H.; Shaik, S.; Yao, J. N. *J. Chem. Theory Comput.* **2011**, *7*, 4002−4011.
(73) Kang, R. H.; Lai, W. Z.; Yao, J. N.; Shaik, S.; Chen, H. *J. Chem. Theory Comput.* **2012**, *8*, 3119−3127.
(74) Lai, W. Z.; Yao, J. N.; Shaik, S.; Chen, H. *J. Chem. Theory Comput.* **2012**, *8*, 2991−2996.
(75) Kang, R. H.; Yao, J. N.; Chen, H. *J. Chem. Theory Comput.* **2013**, *9*, 1872−1879.
(76) Sun, Y. Y.; Chen, H. *J. Chem. Theory Comput.* **2013**, *9*, 4735−4743.
(77) Kim, J.; Ihee, H.; Lee, Y. S. *J. Chem. Phys.* **2010**, *133*, 144309.
(78) Zhao, S.; Li, Z. H.; Wang, W. N.; Liu, Z. P.; Fan, K. N.; Xie, Y. M.; Schaefer, H. F. *J. Chem. Phys.* **2006**, *124*, 184102.
(79) Bartlett, R. J.; Musiał, M. *Rev. Mod. Phys.* **2007**, *79*, 291−352.

(80) (a) Persson, B. J.; Taylor, P. R. *Theor. Chem. Acc.* **2003**, *110*, 211−217. (b) Balabanov, N. B.; Peterson, K. A. *J. Chem. Phys.* **2006**, *125*, 074110. (c) Figgen, D.; Peterson, K. A.; Stoll, H. *J. Chem. Phys.* **2008**, *128*, 034110. (d) Peterson, K. A.; Puzzarini, C. *Theor. Chem. Acc.* **2005**, *114*, 283−296. (e) Figgen, D.; Peterson, K. A.; Dolg, M.; Stoll, H. *J. Chem. Phys.* **2009**, *130*, 164108. (f) Figgen, D.; Rauhut, G.; Dolg, M.; Stoll, H. *Chem. Phys.* **2005**, *311*, 227−244. (g) Harvey, J. N. *J. Biol. Inorg. Chem.* **2011**, *16*, 831−839.
(81) Hattig, C.; Klopper, W.; Kohn, A.; Tew, D. P. *Chem. Rev.* **2012**, *112*, 4−74.
(82) (a) Knizia, G.; Adler, T. B.; Werner, H.-J. *J. Chem. Phys.* **2009**, *130*, 054104. (b) Adler, T. B.; Knizia, G.; Werner, H.-J. *J. Chem. Phys.* **2007**, *127*, 221106.
(83) Peterson, K. A.; Figgen, D.; Dolg, M.; Stoll, H. *J. Chem. Phys.* **2007**, *126*, 124101.
(84) Dunning, T. H., Jr. *J. Chem. Phys.* **1989**, *90*, 1007−1023.
(85) Bühl, M.; Reimann, C.; Pantazis, D. A.; Bredow, T.; Neese, F. *J. Chem. Theory Comput.* **2008**, *4*, 1449−1459.
(86) Werner, H.-J.; Knowles, P. J.; Lindh, R.; Manby, F. R.; Schütz, M.; Celani, P.; Korona, T.; Mitrushenkov, A.; Rauhut, G.; Adler, T. B.; Amos, R. D.; Bernhardsson, A.; Berning, A.; Cooper, D. L.; Deegan, M. J. O.; Dobbyn, A. J.; Eckert, F.; Goll, E.; Hampel, C.; Hetzer, G.; Hrenar, T.; Knizia, G.; Köppl, C.; Liu, Y.; Lloyd, A. W.; Mata, R. A.; May, A. J.; McNicholas, S. J.; Meyer, W.; Mura, M. E.; Nicklass, A.; Palmieri, P.; Pflüger, K.; Pitzer, R.; Reiher, M.; Schumann, U.; Stoll, H.; Stone, A. J.; Tarroni, R.; Thorsteinsson, T.; Wang, M.; Wolf, A. *MOLPRO*, version 2010.1, a package of ab initio programs; see http://www.molpro.net.
(87) (a) Adler, T. B.; Werner, H.-J. *J. Chem. Phys.* **2011**, *135*, 144117. (b) Kong, L.; Bischoff, F. A.; Valeev, E. F. *Chem. Rev.* **2012**, *112*, 75−107.
(88) Schwenke, D. W. *J. Chem. Phys.* **2005**, *122*, 014107.
(89) Hill, J. G.; Peterson, K. A.; Knizia, G.; Werner, H.-J. *J. Chem. Phys.* **2009**, *131*, 194105.
(90) Knizia, G.; Werner, H.-J. *J. Chem. Phys.* **2008**, *128*, 154103.
(91) Martin, J. M. L. *Chem. Phys. Lett.* **1996**, *259*, 669−678.
(92) Feller, D.; Peterson, K. A.; Hill, J. G. *J. Chem. Phys.* **2011**, *135*, 044102.
(93) (a) Weigend, F. *J. Comput. Chem.* **2008**, *29*, 167−175. (b) The def2-AQZVPP/JKFIT basis set contains one even-tempered diffuse function for each primitive set of Weigend's def2-QZVPP/JKFIT in ref 93a and was taken from the Molpro basis set library.
(94) (a) Weigend, F. *Phys. Chem. Chem. Phys.* **2002**, *4*, 4285−4291. (b) The aug-cc-pVTZ/JKFIT basis set contains one even-tempered diffuse function for each primitive set of Weigend's cc-pVTZ/JKFIT in ref 94a and was taken from the Molpro basis set library.
(95) Hill, J. G. *J. Chem. Phys.* **2011**, *135*, 044105.
(96) Weigend, F.; Köhn, A.; Hättig, C. *J. Chem. Phys.* **2002**, *116*, 3175−3183.
(97) Valeev, E. F. *Chem. Phys. Lett.* **2004**, *395*, 190−195.
(98) Hill, J. G.; Peterson, K. A. *J. Chem. Theory Comput.* **2012**, *8*, 518−526.
(99) Frisch, M. J.; Trucks, G. W.; Schlegel, H. B.; Scuseria, G. E.; Robb, M. A.; Cheeseman, J. R.; Scalmani, G.; Barone, V.; Mennucci, B.; Petersson, G. A.; Nakatsuji, H.; Caricato, M.; Li, X.; Hratchian, H. P.; Izmaylov, A. F.; Bloini, J.; Zheng, G.; Sonnenberg, J. L.; Hada, M.; Ehara, M.; Toyota, K.; Fukuda, R.; Hasegawa, J.; Ishida, M.; Nakajima, T.; Honda, Y.; Kitao, O.; Nakai, H.; Vreven, T.; Montgomery, J. A., Jr.; Peralta, J. E.; Ogliaro, F.; Bearpark, M.; Heyd, J. J.; Brothers, E.; Kudin, K. N.; Staroverov, V. N.; Kobayashi, R.; Normand, J.; Raghavachari, K.; Rendell, A.; Burant, J. C.; Iyengar, S. S; Tomasi, J.; Cossi, M.; Rega, N.; Millam, J. M.; Klene, M.; Knox, J. E.; Cross, J. B.; Bakken, V.; Adamo, C.; Jaramillo, J.; Comperts, R.; Stratmann, R. E.; Yazyev, O.; Austin, A. J.; Cammi, R.; Pomelli, C.; Ochterski, J. W.; Martin, R. L.; Morokuma, K.; Zakrzewski, V. G.; Voth, G. A.; Salvador, P.; Dannenbuerg, J. J.; Dapprich, S.; Daniels, A. D.; Farkas, O.; Foresman, J. B.; Ortiz, J. V.; Cioslowski, J.; Fox, D. J. *Gaussian 09*, revision C.01; Gaussian, Inc.: Wallingford, CT, 2009.
(100) (a) Perdew, J. P.; Burke, K.; Ernzerhof, M. *Phys. Rev. Lett.* **1996**, *77*, 3865−3868. (b) Ernzerhof, M.; Scuseria, G. E. *J. Chem. Phys.* **1999**, *110*, 5029−5036. (c) Adamo, C.; Barone, V. *J. Chem. Phys.* **1999**, *110*, 6158−6170.
(101) (a) Zhao, Y.; Truhlar, D. G. *J. Chem. Phys.* **2006**, *125*, 194101. (b) Zhao, Y.; Truhlar, D. G. *Theor. Chem. Acc.* **2008**, *120*, 215−241.
(102) Tao, J.; Perdew, J. P.; Staroverov, V. N.; Scuseria, G. E. *Phys. Rev. Lett.* **2003**, *91*, 146401.
(103) (a) Becke, A. D. *Phys. Rev. A* **1988**, *38*, 3098−3100. (b) Lee, C.; Yang, W.; Parr, R. G. *Phys. Rev. B* **1988**, *37*, 785−789. (c) Becke, A. D. *J. Chem. Phys.* **1993**, *98*, 5648−5652.
(104) Karton, A.; Tarnopolsky, A.; Lamere, J.-F.; Schatz, G. C.; Martin, J. M. L. *J. Phys. Chem. A* **2008**, *112*, 12868−12886.
(105) Grimme, S. *J. Chem. Phys.* **2006**, *124*, 034108.
(106) Chai, J.-D.; Head-Gordon, M. *J. Chem. Phys.* **2008**, *128*, 084106.
(107) Handy, N. C.; Cohen, A. J. *Mol. Phys.* **2001**, *99*, 403−412.
(108) Boese, A. D.; Martin, J. M. L. *J. Chem. Phys.* **2004**, *121*, 3405−3416.
(109) Perdew, J. P. *Phys. Rev. B* **1986**, *33*, 8822−8824.
(110) Yanai, T.; Tew, D.; Handy, N. *Chem. Phys. Lett.* **2004**, *393*, 51−57.
(111) (a) Vydrov, O. A.; Heyd, J.; Krukau, A. V.; Scuseria, G. E. *J. Chem. Phys.* **2006**, *125*, 074106. (b) Vydrov, O. A.; Scuseria, G. E. *J. Chem. Phys.* **2006**, *125*, 234109.
(112) Grimme, S.; Antony, J.; Ehrlich, S.; Krieg, H. *J. Chem. Phys.* **2010**, *132*, 154104.
(113) Goerigk, L.; Grimme, S. *J. Chem. Theory Comput.* **2011**, *7*, 291−309.
(114) Chai, J.-D.; Head-Gordon, M. *Phys. Chem. Chem. Phys.* **2008**, *10*, 6615−6620.
(115) Chen, K. J.; Zhang, G. L.; Chen, H.; Yao, J. N.; Danovich, D.; Shaik, S. *J. Chem. Theory Comput.* **2012**, *8*, 1641−1645.